BRIEF COMMUNICATION OPEN

Check for updates

Biallelic *ATP2B1* variants as a likely cause of a novel neurodevelopmental malformation syndrome with primary hypoparathyroidism

Patrick Yap[1,2✉], Lisa G. Riley[3,4], Purvi M. Kakadia[1,5], Stefan K. Bohlander[1,5], Ben Curran[1], Meer Jacob Rahimi[6], Salam Alburaiky[2], Ian Hayes[2], Henry Oppermann[6], Cristin Print[1], Sandra T. Cooper[4,7,8,9] and Polona Le Quesne Stabej[1,9]

ATP2B1 encodes plasma membrane calcium-transporting-ATPase1 and plays an essential role in maintaining intracellular calcium homeostasis that regulates diverse signaling pathways. Heterozygous de novo missense and truncating *ATP2B1* variants are associated with a neurodevelopmental phenotype of variable expressivity. We describe a proband with distinctive craniofacial gestalt, Pierre-Robin sequence, neurodevelopmental and growth deficit, periventricular heterotopia, brachymesophalangy, cutaneous syndactyly, and persistent hypocalcemia from primary hypoparathyroidism. Proband-parent trio exome sequencing identified compound heterozygous *ATP2B1* variants: a maternally inherited splice-site (c.3060+2 T > G) and paternally inherited missense c.2938 G > T; p.(Val980Leu). Reverse-transcription-PCR on the proband's fibroblast-derived mRNA showed aberrantly spliced *ATP2B1* transcripts targeted for nonsense-mediated decay. All correctly-spliced *ATP2B1* mRNA encoding p.(Val980Leu) functionally causes decreased cellular Ca^{2+} extrusion. Immunoblotting showed reduced fibroblast ATP2B1. We conclude that biallelic *ATP2B1* variants are the likely cause of the proband's phenotype, strengthening the association of *ATP2B1* as a neurodevelopmental gene and expanding the phenotypic characterization of a biallelic loss-of-function genotype.

European Journal of Human Genetics (2024) 32:125–129; https://doi.org/10.1038/s41431-023-01484-9

INTRODUCTION

ATP2B1 encodes the plasma membrane calcium-transporting ATPase 1 (ATP2B1 or PMCA1), which regulates intracellular Ca^{2+} concentration by Ca^{2+} extrusion. Mammals express four Plasma Membrane Calcium ATPases (ATP2B1-4) encoded by four genes (*ATP2B1-4*). Targeted deletions of *Atp2b1-4* in mice show distinct phenotypes, highlighting the functional specificity of each gene [1, 2]. *ATP2B1* is expressed ubiquitously and is the earliest isoform expressed in embryonic development [3]. Homozygous *Atp2b1* knockout (ko) mouse is embryonically lethal before organogenesis [4, 5], whereas heterozygous *Atp2b1-ko* mice have hypertension, hypocalcemia with decreased intact parathyroid hormone (PTH) levels, and increased bone mineral density [6]. Calcium plays an important role in cellular signaling and physiological functions, from bone mineralization, and cardiac and vascular muscle contraction, to early stages of embryonic neurogenesis, synaptogenesis, neurotransmission and their regulation [7]. In humans, single nucleotide polymorphisms in *ATP2B1* have been implicated as risk factors for essential hypertension; [8] this was underpinned by vascular smooth muscle cell-specific *Atp2b1*-ko mice which showed significantly higher systolic blood pressure with increased intracellular calcium concentration [9]. Rahimi et al. recently reported twelve patients harboring heterozygous *ATP2B1* missense or truncating variants, manifesting mild to moderate global developmental delay. The authors proposed haploinsufficiency as the disease-causing mechanism [10]. Functional Ca^{2+} imaging in cells transfected with *ATP2B1* missense variants showed significantly decreased Ca^{2+} extrusion capacity, providing compelling evidence implicating *ATP2B1* in the pathogenesis of a neurodevelopmental phenotype due to dysregulation of Ca^{2+} homeostasis and signaling [10].

MATERIALS AND METHODS

Exome sequencing and analysis

Genomic DNA was extracted from peripheral blood via standard protocols. Whole exome sequencing was performed with Agilent SureSelect Clinical Research Exome V1 (Santa Clara, CA, USA) on NextSeq500 (Illumina, CA, USA) (Supporting Methods).

Splicing RNA experiments, Western blot and $[Ca^{2+}]_i$ imaging are described in Supporting Methods.

[1]Department of Molecular Medicine and Pathology, University of Auckland, Auckland, New Zealand. [2]Genetic Health Service New Zealand - Northern hub, Auckland, New Zealand. [3]Rare Diseases Functional Genomics, Kids Research, The Children's Hospital at Westmead and The Children's Medical Research Institute, Sydney, NSW 2145, Australia. [4]Specialty of Child & Adolescent Health, Sydney Medical School, University of Sydney, Sydney, NSW 2006, Australia. [5]Leukaemia and Blood Cancer Research Unit, Department of Molecular Medicine and Pathology, University of Auckland, Auckland, New Zealand. [6]Institute of Human Genetics, University of Leipzig Hospitals and Clinics, Leipzig 04103, Germany. [7]Kids Neuroscience Centre, Kids Research, Children's Hospital at Westmead, Sydney, NSW 2145, Australia. [8]The Children's Medical Research Institute, 214 Hawkesbury Road, Westmead, NSW 2145, Australia. [9]These authors contributed equally: Sandra T. Cooper, Polona Le Quesne Stabej. ✉email: patricky@adhb.govt.nz

Received: 2 February 2023 Revised: 22 August 2023 Accepted: 10 October 2023
Published online: 6 November 2023

Table 1. Serum concentration of calcium metabolism indices in the proband and parents.

Assay	Reference interval	Proband				Mother	Father
		Neonate	6 y	10 y	14 y		
Calcium (adjusted)	2.10–2.55 mmol/L	1.70	2.01	2.05	2.05	2.10–2.20	2.34
Intact-Parathyroid Hormone (iPTH)	3.00–8.50 pmol/L	NA	1.85	3.00	3.00	6.00	4.00

NA not available, *y* years.

RESULTS

The male (46,XY) proband was born to healthy, non-consanguineous European parents. Cleft palate, micro-retrognathia, unilateral (left) fixed talipes equinovarus, and intermittent stridor were documented at birth. Growth parameters at birth were normal (p25-75) for weight, length, and occipitofrontal circumference (OFC). CGH-array (Affymetrix CytoScan, hg19) did not detect clinically significant genomic imbalances. Detailed phenotyping in early childhood reveals asymmetrical growth deficiency (OFC p50, weight and height p2-10) and distinctive craniofacial appearance characterized by bitemporal narrowing, short palpebral fissures, periorbital fullness, pinched nose, long philtrum, microstomia, bifid uvula, full-saggy cheeks, and micro-retrognathia (Supplementary Fig. S1A, B). Musculoskeletal manifestation includes pectus carinatum, a shortened left Achilles tendon, bilateral brachydactyly with bulbous fingertips, fifth-finger clinodactyly, and flexion deformity of the distal interphalangeal joint of the third and fourth fingers. He has similar digital appearances of the feet with bilateral fourth and fifth-toe syndactyly (Supplementary Fig. S1C–E). Radiographs of the hand show brachymesophalangy (brachydactyly type-A4), characterized by under-modelled phalanges with irregular metaphyses. The middle phalanges of the fifth and index fingers appear dysplastic, resembling an angel-shape phalanx (Supplementary Fig. S1F, G). He was diagnosed with moderate intellectual disability; WISC-IV-Full Scale Intelligence Quotient score of 50 and significantly impaired adaptive functioning. Brain magnetic resonance imaging (MRI) showed periventricular nodular heterotopia (PVNH) in the left lateral ventricle. There is no record of epilepsy.

In retrospect, subclinical hypocalcemia was recorded in the neonatal period and at ten and fourteen years of age (Table 1). Secondary hyperphosphatemia was evident from school age. He maintains a normal renal function. Intact-Parathyroid hormone (iPTH) levels were in the lower limit of normal despite hypocalcemia. Serum magnesium and urinary calcium and phosphate levels were normal. Electroencephalograms, renal ultrasonography, echocardiogram, and ophthalmological assessments were unremarkable. Autism Diagnostic Observation Schedule 2 (ADOS-2) assessment indicates a low likelihood of autism. Recorded systolic and diastolic blood pressure measurements are within the normal limits for age and height. The proband's parents are phenotypically normal with no history of neurodevelopmental deficit or hypertension. The mother has low-normal adjusted calcium, and normal phosphate and PTH levels. These are normal in the father (Table 1).

Exome data analysis

Exome variant analysis using de novo, autosomal-dominant (inherited from mosaic parent), X-linked and autosomal-recessive (homozygous) models did not detect any variants relevant to proband's phenotype. Applying an autosomal-recessive compound heterozygous filter, *ATP2B1* variants were identified: maternally-inherited canonical splice-site variant (GRCh37/NC_000012.11:g.89996818 A > C; NM_001366521.1:c.3060+2 T > G) in intron 18 and paternally-inherited missense (GRCh37/NC_000012.11:g.89996942 C > A; NM_001366521.1:c.2938 G > T,p.(Val980Leu)) in exon 18 which encodes the transmembrane domain 8 (Fig. 1A). Both variants are absent or extremely rare in the population and disease databases (Supplementary Table S3).

Functional consequences of ATP2B1 variants

ATP2B1 cDNA analysis from proband's fibroblasts demonstrates that the c.3060+2 T > G variant induces multiple abnormal splicing events likely resulting in nonsense-mediated decay (Fig. 1B, C and Supporting Results). Western blot analyses on proband's fibroblast lysate showed a significant reduction of full-length (135 kDa) ATP2B1 to approximately 20% (Fig. 1D, E and Supporting Results). $[Ca^{2+}]_i$ imaging experiments revealed p.(Val980Leu) causes decreased cellular Ca^{2+} extrusion compared to the wild type (Fig. 2).

Collective results from our functional studies indicate the mechanism for the disease is due to loss of canonically spliced transcripts from the maternal allele and reduced levels of a dysfunctional ATP2B1 p.(Val980Leu) from the paternal allele.

DISCUSSION

We describe the first case of biallelic, compound heterozygous *ATP2B1* variants in a proband with a neurodevelopmental phenotype, characterized by distinctive craniofacial and skeletal features, and persistent hypocalcemia due to primary hypoparathyroidism. The Genome Aggregation Database (gnomAD) shows *ATP2B1* is highly intolerant to genetic variation, depleted in both loss-of-function (pLI score of 1) and missense variants (*Z*-score 5.29). Global germline knockout of *Atp2b1* in mice is associated with embryonic lethality [4, 5]. There is a strong association between lethal murine recessive knockouts and genes linked to severe phenotypes in humans, with 75% of known prenatal-lethal genes in humans linked to developmentally lethal phenotypes in mice [11].

Murine studies establish marked surges in *Atp2b1* expression during embryogenesis at the early stage of differentiation into neural progenitor cells, during mitosis and later stages of neural tube formation, postulated to promote neural tube closure in neuronal migration [7, 12]. It is therefore plausible that significant disruption of *ATP2B1* function in human brain predisposes to a neurodevelopmental and malformation phenotype. PVNH is a well-described entity of disordered neuronal migration. The manifestation of partial PVNH in the proband strengthens the hypothesis that *ATP2B1* plays an essential role in the early stages of neurogenesis and PVNH as a phenotypic spectrum of the proposed neurodevelopmental malformation syndrome. Ten out of twelve probands with monoallelic (de novo) *ATP2B1* variants described by Rahimi et al. [10], are reported to have normal brain imaging. Imaging findings described in the remaining two individuals are not indicative of neuronal migration disorders (cerebral cavernoma and isolated ventriculomegaly).

We compare and contrast the phenotypic features of individuals with monoallelic and biallelic pathogenic *ATP2B1* variants. We included the phenotypic data of seven individuals recorded on Decipher, heterozygous for de novo copy number variants; deletions sized 5.3–101 Mb, encompassing *ATP2B1*. Although the phenotypes in individuals with deletions are more likely to represent the effect of the contiguous-gene deletion, we are able to identify and exclude phenotypic features less likely to be

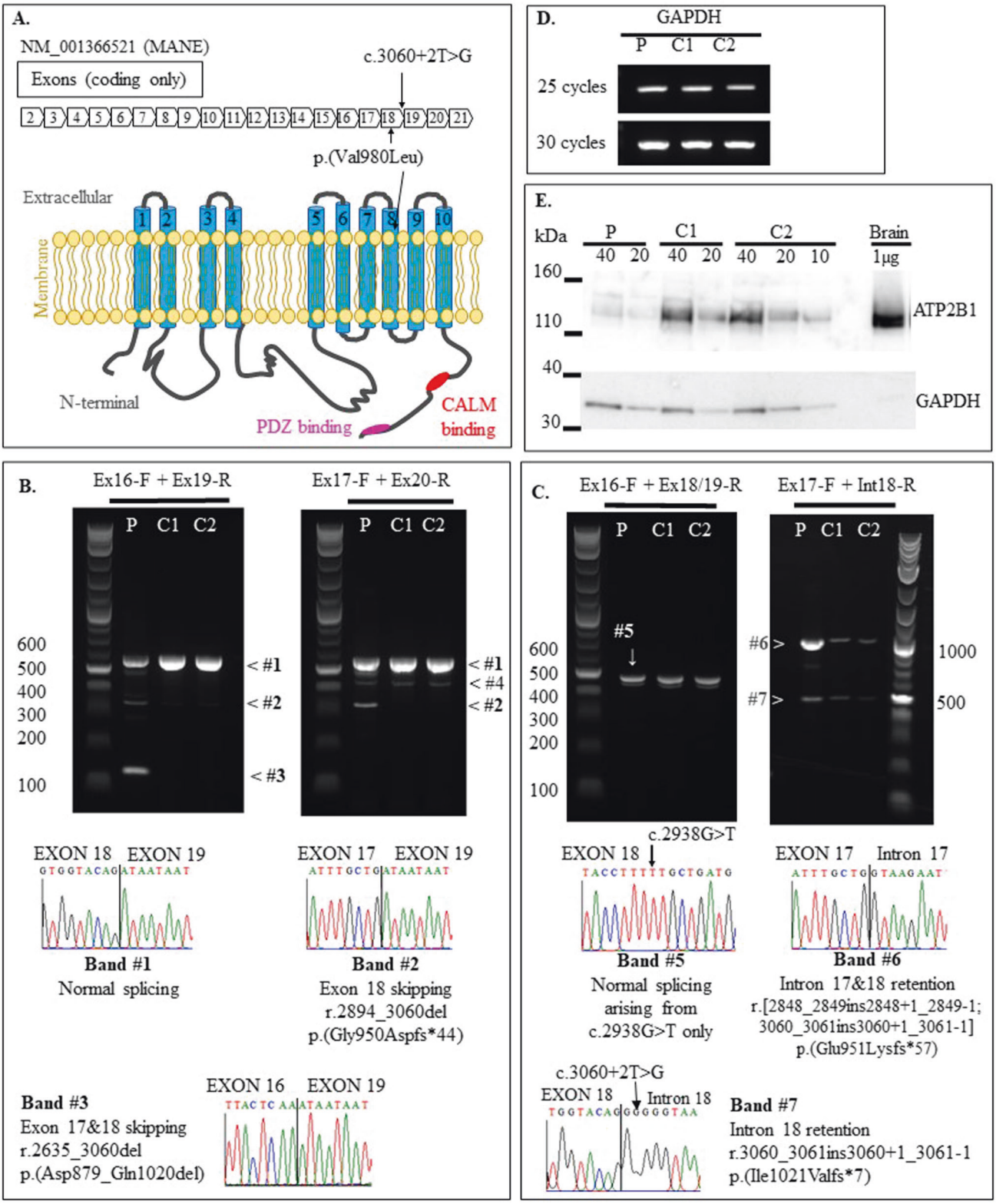

attributed to *ATP2B1*. The phenotypic analysis demonstrated some overlap, as well as delineated the distinguishing distinctive features in the monoallelic and biallelic cohorts. We identified the phenotypic features specific for the biallelic loss-of-function effect, which includes PVNH, Pierre-Robin sequence, primary hypoparathyroidism, brachymesophalangy, and a distinctive craniofacial gestalt. (Supplementary Table S5)

While the conspicuous neurodevelopmental deficit in the proband with biallelic *ATP2B1* variants overlaps with the global developmental delay (mild to moderate) observed in the de novo monoallelic cohort [10], the parents of our proband, heterozygous for pathogenic *ATP2B1* variants do not show overt clinical symptoms, including the c.3060+2 T > G variant carrier mother. Pre-mRNA splicing studies indicate c.3060+2 T > G is associated

Fig. 1 ATP2B1 gene/protein diagram and abnormal splicing events induced by c.3060+2T > G. A. Schematic diagram showing location of ATP2B1:c.2938G > T in exon 18 and c.3060+2T > G in intron 18. Ten transmembrane domains, calmodulin (CALM), and PDZ binding domains are depicted in ATP2B1 protein. **B** Splicing effects of ATP2B1 c.3060+2 T > G. RT-PCR amplicons (RNA from proband's fibroblasts) using two sets of primers (Ex16-F + Ex19-R; Ex17-F + Ex20-R) flanking the c.3060+2 T > G variant (intron 18), we detect two abnormally sized bands in the proband: Band#2 (exon 18 skipping; r.2849_3060del, p.(Gly950Aspfs*44)) and #3 (exon 17–18 skipping; r.2635_3060del, p.(Asp879_Gln1020del)). **C** Using forward primer in exon 16 (Ex16-F) and reverse that flanks exon 18-exon 19 boundary (Ex18/19-R), we detect normally spliced Band#5; Sanger sequencing of proband's Band#5 established that all normally spliced ATP2B1 transcripts contain c.2983 G > T, p.(Val980Leu) variant only. Using a forward primer in exon 17 (Ex17-F) and reverse in intron 18 (In18-R) we detect increased levels of intron 18 retention (Band#7; r.3060_3061ins3060 + 1_3061-1, p.(Ile1021Valfs*7)) and intron 17&18 retention (Band#6; r.[2848_2849ins2848 + 1_2849-1;3060_3061ins3060 + 1_3061-1], p.(Glu951Lysfs*57)) in proband relative to two controls. All proband's splice transcripts with intron 18 retention contained splice variant c.3060+2 T > G (Band#7 Sanger sequence) **D** Amplification of GAPDH demonstrates cDNA loading. **E** Western blot of patient and control fibroblasts showing ATP2B1 protein levels. 10–40 µg of fibroblast lysate was loaded. Human brain was used as a positive control. GAPDH was used as a loading control. Image is representative of three independent experiments. Lanes: Proband (P) Control 1 (C1), Control 2 (C2).

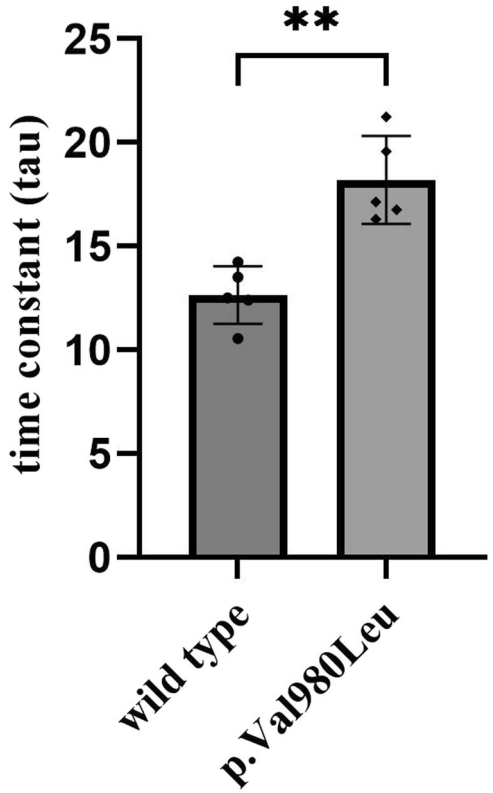

Fig. 2 Time-dependent $[Ca^{2+}]_i$ decline of p.(Val980Leu) transfected HEK293 was analysed after final addition of EGTA that is represented by the time constant tau. Data presented as mean and standard deviation from five independent experiments; $^{**}p = 0.0012$.

with multiple mis-splicing events, all resulting in probable loss-of-function (encoded premature termination codons or deletion of multiple transmembrane domains). Western blot did not identify any potentially part-functional, truncated ATP2B1 isoforms in fibroblasts from the proband. Three individuals in the cohort described by Rahimi et al., harbor heterozygous truncating *ATP2B1* variants; two with unknown inheritance (c.458 G > A; p.(Trp153*), c.1789C>T; p.(Arg597*)) and one (c.2632 C > T, p.(Gln878*)) confirmed de novo in a patient with motor and speech delay, hyperactivity, normal growth, sparse eyebrow and palpebral edema. Based on the analyses of the NGS and Sanger sequencing data in our study, the proband's parents were non-mosaic for *ATP2B1* variants (variant allele frequencies were 58%) in the father (c.2938 G > T; p.(Val980Leu)) and 50% in the mother (c.3060+2 T > G). In the absence of mosaicism in the parents, the mechanism behind monoallelic missense and truncating *ATP2B1* variants leading to the phenotypes described remains speculative.

The functional evidence of monoallelic pathogenic *ATP2B1* variants in altering intracellular calcium homeostasis is indisputable. Functional Ca^{2+} imaging data indicates the p.(Val980Leu) variant has a clear deleterious impact on the ATP2B1 function (*tau*-value:18.2; wild-type: 12.64). Rahimi et al. in their publication identified p.(Arg991Gln) and p.(His459Arg) as the high and low-impact variants, respectively. The corresponding *tau*-values were 23.92 and 17.79 [10]. Based on the *tau*-value, p.(Val980Leu) is predicted a low-impact variant. The correlation between *tau*-value and phenotypic severity is not yet delineated. The clinical manifestation in heterozygous carriers of loss-of-function autosomal recessive alleles is likely to be highly variable. The low impact p.(Val980Leu) variant and variable expressivity provide a plausible explanation for the phenotypically unaffected parents harboring heterozygous pathogenic *ATP2B1* variants.

In conclusion, we provide a detailed phenotypic characterization of a biallelic *ATP2B1* disorder, in a proband manifesting a distinctive neurodevelopmental, craniofacial, and skeletal phenotype, and persistent hypocalcemia secondary to primary hypoparathyroidism, discernible from other well-described syndromes (Supplementary Table S2). We provide functional evidence from RNA and protein studies, and functional Ca^{2+} imaging, confirming the deleterious effects of the compound heterozygous *ATP2B1* variants. We postulate a likely critical threshold for retained functional ATP2B1 protein that enables survival and pathogenesis of the clinical phenotype. We have not identified another proband with biallelic *ATP2B1* variants through GeneMatcher [13] and other disease databases. We consider that surviving, manifesting probands with biallelic *ATP2B1* variants may be rare. Detailed phenotyping of more cases with confirmed genotype may delineate and expand the phenotypic and genotypic spectrum of monoallelic and biallelic *ATP2B1*-related disorders, providing insights into the critical role of ATP2B1 in human development.

Web resources

ClinVar database: https://www.ncbi.nlm.nih.gov/clinvar/ (accessed July 15, 2022)

Genome Aggregation Database (gnomAD): http://gnomad.broadinstitute.org/ (accessed July 15, 2022)

NHLBI Exome Sequencing project (ESP): https://evs.gs.washington.edu/ (accessed July 15, 2022)

Missense3D-DB: http://missense3d.bc.ic.ac.uk/ (accessed July 15, 2022)

Geno2MP: https://geno2mp.gs.washington.edu/Geno2MP (accessed July 15, 2022)

MyGene2: https://www.mygene2.org/MyGene2/ (accessed July 15, 2022)

Decipher: https://www.deciphergenomics.org/ddd/ (accessed July 15, 2022)

Decipher: https://www.deciphergenomics.org/gene/ATP2B1/patient-overlap/cnvs (accessed June 1, 2023)

Global Variome shared LOVD-ATP2B1: https://databases.lovd.nl/shared/variants/ATP2B1 (accessed July 15, 2022)

International Mouse Phenotyping Consortium (IMPC): https://www.mousephenotype.org/data/genes/MGI:104653 (accessed July 15, 2022)

DATA AVAILABILITY

The accession numbers for identified *ATP2B1* variants were deposited in ClinVar (https://www.ncbi.nlm.nih.gov/clinvar/) with the following identifiers: SCV002061315 and SCV002061316. We do not have patient consent to release raw next generation sequencing data.

REFERENCES

1. Strehler EE. Plasma membrane calcium ATPases as novel candidates for therapeutic agent development. J Pharm Pharm Sci a Publ Can Soc Pharm Sci Soc Can des Sci Pharm. 2013;16:190–206.
2. Street VA, McKee-Johnson JW, Fonseca RC, Tempel BL, Noben-Trauth K. Mutations in a plasma membrane Ca2+-ATPase gene cause deafness in deafwaddler mice. Nat Genet. 1998;19:390–4.
3. Chen J, Sitsel A, Benoy V, Sepúlveda MR, Vangheluwe P. Primary active Ca(2+) transport systems in health and disease. Cold Spring Harb Perspect Biol. 2020;12:a035113.
4. Okunade GW, Miller ML, Pyne GJ, Sutliff RL, O'Connor KT, Neumann JC, et al. Targeted ablation of plasma membrane Ca2+-ATPase (PMCA) 1 and 4 indicates a major housekeeping function for PMCA1 and a critical role in hyperactivated sperm motility and male fertility for PMCA4. J Biol Chem. 2004;279:33742–50.
5. Dickinson ME, Flenniken AM, Ji X, Teboul L, Wong MD, White JK, et al. High-throughput discovery of novel developmental phenotypes. Nature 2016;537:508–14.
6. Ehara Y, Hirawa N, Sumida K, Fujiwara A, Kagimoto M, Ooki-Okuyama Y, et al. Reduced secretion of parathyroid hormone and hypocalcemia in systemic heterozygous ATP2B1-null hypertensive mice. Hypertens Res. 2018;41:699–707.
7. Bouron A. Transcriptomic profiling of Ca2+ transport systems during the formation of the cerebral cortex in mice. Cells 2020;9:1800.
8. Levy D, Ehret GB, Rice K, Verwoert GC, Launer LJ, Dehghan A, et al. Genome-wide association study of blood pressure and hypertension. Nat Genet. 2009;41:677–87.
9. Kobayashi Y, Hirawa N, Tabara Y, Muraoka H, Fujita M, Miyazaki N, et al. Mice lacking hypertension candidate gene ATP2B1 in vascular smooth muscle cells show significant blood pressure elevation. Hypertension 2012;59:854–60.
10. Rahimi MJ, Urban N, Wegler M, Sticht H, Schaefer M, Popp B, et al. De novo variants in ATP2B1 lead to neurodevelopmental delay. Am J Hum Genet. 2022;109:944–52.
11. Dawes R, Lek M, Cooper ST. Gene discovery informatics toolkit defines candidate genes for unexplained infertility and prenatal or infantile mortality. NPJ Genom Med. 2019;4:8.
12. Chen M, Laursen SH, Habekost M, Knudsen CH, Buchholdt SH, Huang J, et al. Central and peripheral nervous system progenitors derived from human pluripotent stem cells reveal a unique temporal and cell-type specific expression of PMCAs. Front Cell Dev Biol. 2018;6:5.
13. Sobreira N, Schiettecatte F, Valle D, Hamosh A. GeneMatcher: a matching tool for connecting investigators with an interest in the same gene. Hum Mutat. 2015;36:928–30.

ACKNOWLEDGEMENTS

We thank the family for being part of this study and for their consent to publish their medical information and relevant images in a peer-reviewed journal. We would like to thank Prof Frank Gaunitz (Department of Neurosurgery, University of Leipzig Hospitals and Clinics, Leipzig), Nicole Urban and Prof Michael Schaefer (Rudolf-Boehm-Institute of Pharmacology and Toxicology, University of Leipzig Hospitals and Clinics, Leipzig) for the support of the calcium imaging assays. We thank Pascalene Houseman and Dr Peter Tsai (Molecular medicine and Pathology, University of Auckland) for their contribution in bioinformatic analyses and Dr Dorit Naot (University of Auckland) for helpful discussion.

AUTHOR CONTRIBUTIONS

PY, SA and IH collected and curated clinical data. PMK and SKB performed whole exome sequencing. BC ran bioinformatics data analysis. PLQS performed whole exome variant analysis. PY and PLQS performed variant curation and genotype-phenotype correlation. LR and STC performed mRNA and protein assays. MJR and HO provided data from functional calcium imaging. PY, PLQS, CP and SC wrote the manuscript. PY, CP and PLQS supervised the study. All authors reviewed the final manuscript.

FUNDING

The Genomics Into Medicine (GIM) Strategic Research Initiative at the University of Auckland funded the Ultrarare Syndrome Trio Exome Sequencing Project (HDEC 18/CEN/62) and supported PY (0.2FTE). SKB and PMK are supported by Leukaemia & Blood Cancer New Zealand and the family of Marijana Kumerich. STC is supported by a National Health and Medical Research Council of Australia Senior Research Fellowship (APP1136197). This project has received funding through the Medical Research Future Fund (MRFF) Rapid Applied Research Translation Program grant awarded to Sydney Health Partners. Part of this work was supported by Luminesce Alliance – Innovation for Children's Health. Luminesce Alliance - Innovation for Children's Health, is a not-for-profit cooperative joint venture between the Sydney Children's Hospitals Network, the Children's Medical Research Institute, and the Children's Cancer Institute. It has been established with the support of the NSW Government to coordinate and integrate pediatric research. Luminesce Alliance is also affiliated with the University of Sydney and the University of New South Wales, Sydney. Open Access funding enabled and organized by CAUL and its Member Institutions.

COMPETING INTERESTS

STC is director of Frontier Genomics Pty Ltd (Australia). STC currently receives no consultancy fees or other remuneration for this role. Frontier Genomics Pty Ltd (Australia) has no existing financial relationships that will benefit from publication of these data. All other contributing authors declare no conflict of interest.

ETHICAL APPROVAL

The family was enrolled in a research-based proband-parent trio exome sequencing project for undiagnosed rare syndromes (approved by the Health and Disability Ethics Committee of New Zealand HDEC 18/CEN/62). Written informed consent for publication of images was obtained from the study participants.

ADDITIONAL INFORMATION

Supplementary information The online version contains supplementary material available at https://doi.org/10.1038/s41431-023-01484-9.

Correspondence and requests for materials should be addressed to Patrick Yap.

Reprints and permission information is available at http://www.nature.com/reprints

Publisher's note Springer Nature remains neutral with regard to jurisdictional claims in published maps and institutional affiliations.